ChemComm

COMMUNICATION

Check for updates

Cite this: *Chem. Commun.*, 2024, **60**, 11136

Received 2nd August 2024,
Accepted 2nd September 2024

DOI: 10.1039/d4cc03935a

rsc.li/chemcomm

Facile interconversion of mesitylcopper into a CuMes–Cu_2bis(amidinate) triangle and a tetracuprous Möbius strip†‡

Keri Dowling, §[a] Tomasz Kruczyński,§[a] Sanjay Dutta, [a] D. P. Ngan Le, [b] Samer Gozem, [b] Colin D. McMillen, [c] Nattamai Bhuvanesh [d] and Michael Stollenz *[a]

A new flexible bis(amidine) ligand featuring two additional N-donor groups incorporates a defined $[Cu^{I}MesCu_2^{I}]^{2+}$ fragment from mesitylcopper into a triangular cluster with a reactive organometallic coordination site. Subtle changes to the reaction protocol result in the formation of an intertwined tetracuprous arrangement that adopts the shape of a Möbius strip.

One of the most fascinating topological approaches in synthetic chemistry is the design of molecules that have a one-sided surface with one edge,[1] constructed by inducing an odd number of 180° twists into a circular band structure,[2] which is better known as Möbius band or strip.[3] Möbius strips have been found in various aromatic π systems and related transition states,[1] single-crystalline conductor materials,[4] cyclic antiferromagnetically coupled 3d-metal structures,[5] chiral block copolymers,[6] and have recently been applied in intriguing light-driven actuators.[7] It remains an open question if Möbius topologies of coordination compounds are accessible that lead to other interesting structure-physical property relations, such as the photoluminescence (PL) behavior of transition metal complexes.

Our ongoing interest in photoluminescent Cu^{I} bis(amidinate) clusters forming molecular strings with significant $d^{10}\cdots d^{10}$ contact interactions[8,9] has inspired us to explore new topologies through a systematic variation of the substituents on the polydentate ligand framework. In this communication, we report the synthesis of the first triangular mesitylcopper cluster[10] bearing a single tetradentate chelating ligand and its interconversion into a unique tetracuprous Möbius strip. This Cu^{I}_4 cluster can directly be obtained and isolated by subtle changes on the common reaction protocol.

We have previously demonstrated that flexible *N*,*N*′-disubstituted ethylene-bridged bis(amidines)[11] such as $\mathbf{L^1}H_2$ (Scheme 1) form a series of isostructural binuclear Group 11 metal complexes undergoing additional stabilization through weak N–H···Cl–Au and N–H···$C_{aryl,ipso}$–Au hydrogen bonds, alongside supporting London dispersion forces.[12] We have also observed that tetradentate bis(amidines)[8,13] and mesitylcopper,[14,15] predominantly existing as $[Cu_4Mes_4]$,[14c,15] readily form molecular strings of four cuprous ions as well as clusters with up to ten Cu^{I} centers; all of which serve as potent thermally activated delayed fluorescence (TADF) or phosphorescent emitters.[8,9] The reaction of $\mathbf{L^1}H_2$ and $[Cu_4Mes_4]$ yields an ill-defined, almost insoluble solid, which is presumably a coordination polymer.[16] We hypothesized that the expansion of the alkylene linker to a 1,3-propanediyl bridge ($\mathbf{L^2}H_2$) and subsequent treatment with $[Cu_4Mes_4]$ will result in a more discrete and linear arrangement, due to the unidirectional orientation of the amidine/pyridyl binding sites (Scheme 1). This allows for adjusting two (or more) d^{10} centers in close proximity to each other (< 2.8 Å, the sum of two copper van der Waals radii).[17]

To our surprise, a strictly linear cluster arrangement of four or more Cu^{I} ions was not observed. Instead, $[\mathbf{L^2}]^{2-}$ was revealed to operate as a tailored ligand for a defined triangular mesitylcopper cluster (**1**) and a homoleptic tetranuclear complex (**2**) forming a Möbius strip as thermodynamically preferred arrangement. This was confirmed by single-crystal X-ray diffraction (XRD) for the solid state and supported by density-functional theory (DFT) calculations of the proposed common

[a] *Department of Chemistry and Biochemistry, Kennesaw State University, 370 Paulding Avenue, MD 1203, Kennesaw, Georgia 30144, USA. E-mail: Michael.Stollenz@kennesaw.edu; Web: https://facultyweb.kennesaw.edu/mstollen/*

[b] *Department of Chemistry, Georgia State University, 145 Piedmont Ave SE, Atlanta, Georgia 30303, P. O. Box 3945, Atlanta, Georgia 30302-3945, USA*

[c] *Department of Chemistry, Clemson University, 379 Hunter Laboratories, Clemson, SC 29634-0973, USA*

[d] *Department of Chemistry, Texas A&M University, 580 Ross Street, P.O. Box 30012, College Station, Texas 77842-3012, USA*

† Dedicated to Professor Dr. Dirk Walther on the occasion of his 85th birthday.

‡ Electronic supplementary information (ESI) available: Experimental procedures, computational details, crystallographic data and NMR spectra. CCDC 2373847 ($\mathbf{LH}_2$), 2362330 (**1**) and 2373848 (**2**·C_7H_8). For ESI and crystallographic data in CIF or other electronic format see DOI: https://doi.org/10.1039/d4cc03935a

§ These authors contributed equally to this work.

This journal is © The Royal Society of Chemistry 2024

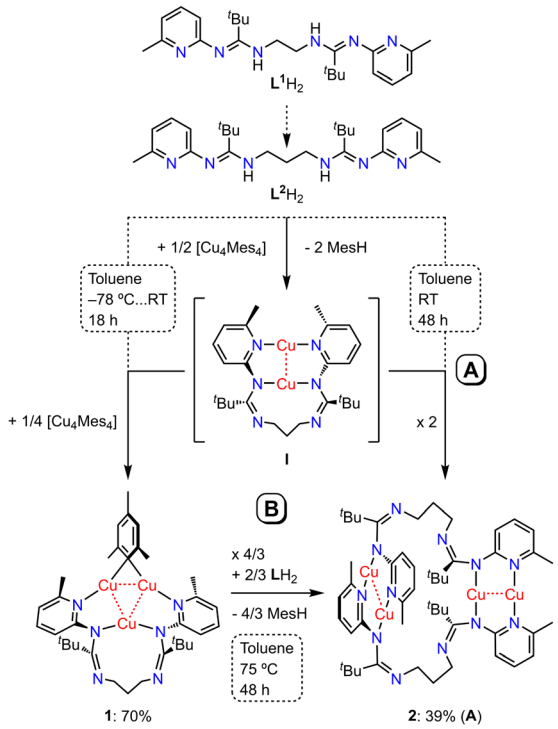

Scheme 1 Synthesis of complexes **1** and **2**.

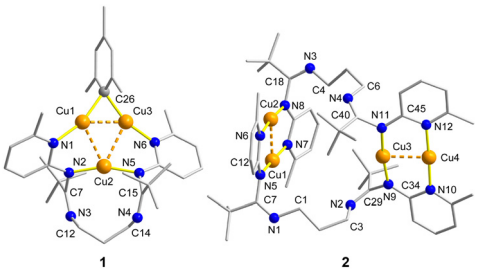

Fig. 1 Solid-state molecular structures of **1** and **2**, determined by XRD. For selected interatomic distances, bond angles, and torsion angles see Fig. S4 and S7, and Table S2 (ESI‡).

intermediate **I** (Scheme 1) as well as alternative isomers of **2** for the gas phase (*vide infra*). ^{1}H, variable-temperature ^{1}H, ^{13}C, and ^{15}N NMR spectra indicate that the molecular structures of **1** and **2** are also retained in solution. PL emission and excitation spectra in solution as well as in solid state of both complexes show very weak to moderate emissions at room temperature, which are significantly increased at temperatures down to 77 K.

Initially, we discovered that $\mathbf{L}^{2}\mathrm{H}_2$ reacts with $[Cu_4Mes_4]$ at low temperature (−78 °C) in toluene solutions to instantly form a yellow precipitate, which was isolated as complex **1** in good yields (up to 70%). The elemental analysis disclosed a stoichiometric ratio of Cu to $[\mathbf{L}^{2}]^{2-}$ to Mes of 3 : 1 : 1. By contrast, more dilute conditions, combined with a slow addition of the $[Cu_4Mes_4]$ solution to $\mathbf{L}^{2}\mathrm{H}_2$ in toluene at room temperature, produced a clear lime green reaction mixture. After workup, complex **2** was obtained as a yellow microcrystalline solid (yield: 39%). Elemental analysis revealed a molecular formula of $[Cu_2\mathbf{L}^{2}]_n$, indicating a homoleptic complex as previously observed for structurally related tetracuprous bis(amidinate) strings.[8,9] Complex formation of **1** and **2** through deprotonation is also indicated by the absence of ν(N–H) stretching frequencies in the IR spectra (Fig. S43–S45, ESI‡).

A single-crystal XRD analysis shows that the unit cell of **1** contains one pair of C_2-symmetrical mirror-image conformations (Fig. S6, ESI‡) and one of them is shown in Fig. 1. The molecular structure of complex **1** comprises one bis(amidinate) ligand $[\mathbf{L}^{2}]^{2-}$ chelating a triangular Cu_3^{I} core cluster that is capped by a mesityl group in a 3c2e^{-} binding mode, similar to the Cu^{I}–C_{ipso}–Cu^{I} Mes bonds in $[Cu_4Mes_4]$[14c,15] and in related dicopper-mesityl units.[10,18–23] The average Cu–C bonding distance in **1** (1.986 Å) is very similar to those examples (*e.g.* 1.993 Å in $[Cu_4Mes_4]\cdot 4THF$,[14c] 1.986 Å in $[Cu_2(N(SiMe_3)_2)_2Cu_2Mes_2]$,[19] or 1.997 Å in $[Cu_4Mes(N(SiMe_3)NMe_2)_3]$[21]). The Cu_3^{I} triangle, consisting of a shorter $[Cu_2Mes]^{+}$ edge and two longer edges defined by three amidinate-bridged Cu^{I} ions, indicates significant $d^{10}\cdots d^{10}$ contact interactions through short distances between the individual cuprous ions (2.4554(11)–2.6006(14) Å).

The coordination of the Cu^{I} centers is accompanied by a rearrangement of the imine bonds of $\mathbf{L}^{2}\mathrm{H}_2$ toward the 1,3-propanediyl-bridged N-donor atoms (for the XRD molecular structure of $\mathbf{L}^{2}\mathrm{H}_2$, see Fig. S1–S3, ESI‡). In contrast to $\mathbf{L}^{2}\mathrm{H}_2$, the distances of the CN bonds adjacent to the 1,3-propanediyl bridge are shorter (1.35 Å on average in $\mathbf{L}^{2}\mathrm{H}_2$ compared to 1.28 Å on average in complex **1**), indicating that they have substantial double bond character, as originally observed in the aryl-substituted CN_2 moieties in $\mathbf{L}^{2}\mathrm{H}_2$. Deprotonation of $\mathbf{L}^{2}\mathrm{H}_2$ and subsequent Cu^{I} coordination allows for the formation of anionic pyridylamido bridging donor groups, which results in the observed double bond rearrangement. This is in consequence of the steric bulk between the ^{t}Bu groups and adjacent CN_2 substituents causing the 6-Me-2-pyridyl groups to adopt an orthogonal orientation to the ^{t}Bu substituents. This orientation impedes sp^{2} hybridization of the pyridyl-substituted CN_2-donor atoms. In conjunction with the steric encumbrance, a rare *ZZ* configuration of a bis(amidine)-based Cu^{I} cluster is observed. This is opposed to typically *EE*-(*anti*,*anti*)[24] configured bis(amidinates) of tetranuclear chain clusters, in which sp^{2} hybridization of both N donor atoms and electron delocalization throughout the amidinate moieties is achieved.[8,9]

The result of the molecular structure determination of **2** by XRD shows one pair of C_2-symmetrical enantiomers and four toluene molecules in the unit cell (Fig. S9, ESI‡). Fig. 1 displays one representative enantiomer. Complex **2** is an unusual intertwined tetranuclear Cu^{I} cluster with two separate binding pockets that are interconnected by two 1,3-propanediyl linkers. One side of **2** features a dicuprous unit that is bridged by two 6-methylpyridylamido sidearms in a parallel fashion. The second binding pocket is similarly generated but now by an antiparallel orientation of the two remaining tethered pyridylamido donor groups. The center of this binding pocket represents the twist point of a Möbius [±1] strip if two imaginary ribbons are constructed that interconnect this twist point with the center of the parallel-arranged dicuprous binding pocket. Each ribbon

coincides with a planar aromatic ring of $[\mathbf{L}^2]^{2-}$, then expands into the planar CN_2 segments, and finally intersects the bridging CH_2 linkers to join the other half of the ribbon from the opposite side of the corresponding ligand. Similar to **1**, the coordination of the Cu^I centers is accompanied by a rearrangement of the original imine bonds of $\mathbf{L}^2H_2$ toward the propylene-bridged N-donor atoms, as indicated by significantly shorter N–CH_2 bonding distances in comparison to $\mathbf{L}^2H_2$ (1.27 Å on average). The Cu···Cu′ contact distances (2.4477(8) Å and 2.4493(9) Å) are comparable to related Cu_4^I bis(amidinate) clusters (2.4398(9)–2.4771(4) Å)[8,9] but are significantly shorter (by ≈ 0.152 Å) than in **1**, in which the bridging $[Cu_2Mes]^+$ segment reinforces sterical constraints. The impact of the mesityl ligand is also reflected by slightly larger Cu–N-pyridyl bonding distances in **1** (by ≈ + 0.027 Å).

Consistent with its solid-state structure, the ^{1}H NMR spectrum of **1** in C_6D_6 shows one set of well-resolved signals and all of them are shifted upfield relative to the free ligand $\mathbf{L}^2H_2$, except for the CH_2 proton resonances (Fig. S24 and S18, ESI‡). The quintet structure of the central methylene proton signal of $\mathbf{L}H_2$ (β) transforms into a multiplet in **1** and shifts downfield by 1.02 ppm. The N–CH_2 resonance (α) splits into a downfield-shifted doublet of triplets (dt) and a multiplet (−0.27 ppm and −0.99 ppm compared to $\mathbf{L}^2H_2$) that are separated by 0.72 ppm from each other, which suggests two non-equivalent α_a and α_b protons at each N–CH_2 group. Since variable-temperature (VT) ^{1}H NMR spectra do not show coalescence up to 75 °C (Fig. S37, ESI‡), the two proton signals indicate a high energy barrier for mutual exchange and therefore a limited flexibility of the 1,3-propanediyl bridge.

The ^{1}H NMR spectrum of **2** in C_6D_6 displays a significantly more complex pattern (Fig. 2).

Due to the different orientations of the 6-Me-2-pyridyl-2-NC(^{t}Bu)N sidearms, two separate sets of resonances for the methyl and ^{t}Bu groups, as well as for the aromatic protons, are observed. In addition, there are six distinct CH_2 signals. Two of them represent two nonequivalent sets of H-atom pairs (β and β') on the central CH_2 groups of the 1,3-propanediyl linkers. Similar to **1**, the α proton signals split into two sets α_a and α_b, which are, attributed to the unsymmetric 1,3-propanediyl chains, complemented by a second pair of α'_a and α'_b sets. Altogether, eight methylene α-H atoms are observed. VT ^{1}H NMR spectroscopy shows that none of these proton signals coalesces (up to 75 °C in C_6D_6, see Fig. S38, ESI‡) and therefore confirms that the solid-state structure of **2** is essentially preserved in solution and is also surprisingly rigid.

The ^{1}H and ^{13}C NMR spectra of **2** in C_6D_6 show additional small signals, both in the aliphatic and aromatic regions, which are not related to impurities or unreacted ligand $\mathbf{L}H_2$. They increase over the course of several hours at room temperature or upon heating (Fig. S39, see also synthetic method B, ESI‡). We tentatively assign most of these signals to two isomers **3** and **4**, which occur in a ratio of **3**:**4**:**2** of ∼1:1:3 and that have antiparallel orientations of the two 6-methylpyridylamido groups at *both* Cu_2^I compartments. This analysis is supported by a (^{1}H, ^{1}H)-ROESY spectrum indicating close proximity between the methyl and ^{t}Bu substituents of **3** and **4**, being consistent with an antiparallel arrangement (Fig. S40, ESI‡). Further evidence is provided by gas-phase DFT calculations on alternative isomers of complex **2** (Fig. S10, ESI‡): **IIa–d** represent feasible isomers (in four conformational arrangements **a–d**) with *two* parallel-coordinated 6-methylpyridylamido sidearms at each dicuprous compartment. The corresponding isomers **III** featuring two *anti*parallel orientations of the N-donor side groups are shown as two conformers **IIIa** and **IIIb** (Fig. 3). The latter are very close (0.42–1.04 kcal mol^{-1}) in free energy to the computationally geometry-optimized structure of **2**, which suggests a possible presence of **IIIa** or **IIIb** alongside **2** in solution. These two isomers are likely similar or even identical to **3** and **4**.

The parallel-arranged isomers **IIa–d**, whose conformational orientations vary by different orientations of the ^{t}Bu substituents to each other, are generally higher in free energy (by up to +12.87 kcal mol^{-1} relative to **2**). The DFT calculation results also support a transient but thermodynamically preferred intermediate **I** (Δ_rG = −29.31 kcal mol^{-1}) that can either undergo insertion of a CuMes unit to form **1** or dimerize into **2** (Scheme 1 and Fig. S10, ESI‡). Relative to **I**, complex **1** is lower in free energy by −12.72 kcal mol^{-1} but is thermodynamically disfavored by +3.34 kcal mol^{-1} in comparison to **2**. This result is consistent with the formation of **1** at lower temperature conditions, facilitated by a quick precipitation, and relatively slow dimerization of the postulated intermediate **I** into **2**. For completion, the corresponding *EE* isomers of **I** and **1**, as well as

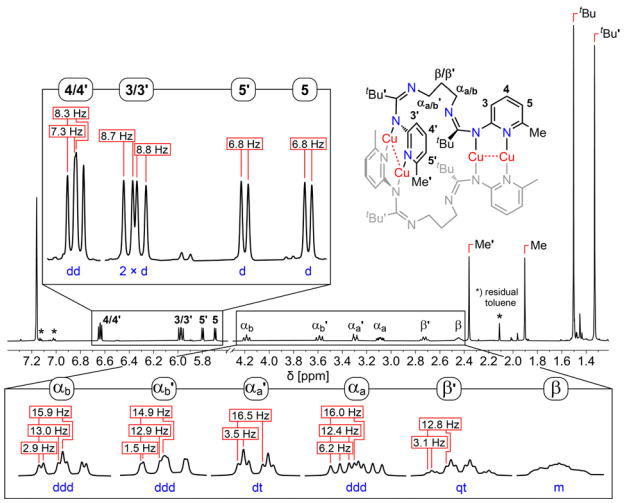

Fig. 2 ^{1}H NMR spectrum of **2** in C_6D_6 (600 MHz).

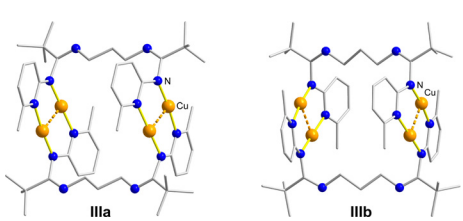

Fig. 3 Computational structures of **IIIa** and **IIIb** (*ZZZZ* isomers).

This journal is © The Royal Society of Chemistry 2024

the *EEEE* isomers of **IIa–d**, **IIIa**, **IIIb**, and **2**, were computationally generated and their relative free energies compared (Scheme S11, ESI‡). As expected from the significantly increased steric constraints imposed by the bulky ^{t}Bu substituents, all *EE* and *EEEE* isomers are considerably higher in free energy than their *ZZ*/*ZZZZ* congeners.

Finally, we investigated the absorption and steady-state PL properties of **1** and **2** (Fig. S49–S60 and Tables S7, S8, ESI‡). Although both complexes are only very weakly emissive in solution (THF, (Φ_f = 0.1% (**1**), 1.0% (**2**))) and show moderate emission in the solid state (Φ_f = 6.9% (**1**), 5.0% (**2**)), both complexes exhibit significantly increased brightness at lower temperatures (150 K in solution and 77 K in the solid state), which suggests restrictions on non-radiative pathways due to reduced intramolecular motion. The large Stokes shifts of **1** and **2** in solution (0.69–0.83 eV) indicate a geometric relaxation of their excited states to significantly different ground state geometries (Table S8, ESI‡) and metal-to-ligand charge transfer (MLCT), as previously observed for related homoleptic Cu^{I} bis(amidinate) clusters.[8] Due to limited space in solids imposed by steric constraints through intermolecular interactions, the Stokes shifts are expectedly smaller in the solid state.

In conclusion, our work has demonstrated that the convenient design of a new *N*,*N*′-disubstituted 1,3-propanediyl-bridged bis(amidine) $\mathbf{L}H_2$ with additional terminal N-donor sites allows for a smooth conversion of the mesitylcopper oligomer into a triangular cluster that retains one reactive CuMes site. Only small changes of the reaction protocol result in the formation of a homoleptic assembly of two interconnected dicuprous compartments that adopts the shape of a Möbius strip as the isomer being the lowest in free energy among feasible alternative array structures. Future studies will address the influence of different ligand substituents on the Cu^{I}-cluster bis(amidinate) topologies and the correlation between their structures and PL properties. We are also interested in investigating the organometallic reactive site of complex **1** and its potential application as a photosensitizer.

We thank Connor Welch for experimental assistance, Prof. Mohammad Halim for assistance on the mass spectrometers, and Prof. Thomas C. Leeper for help on recording ^{15}N HMBC NMR spectra. We gratefully acknowledge computing resources provided by the Advanced Research Computing Technology and Innovation Core (ARCTIC), supported by the US National Science Foundation (CNS-1920024), as well as financial support by the NSF (CHE-1800332 and CHE-2155153) and the College of Sciences and Mathematics at Kennesaw State University.

Data availability

The data supporting this article have been included as part of the ESI.‡

Conflicts of interest

There are no conflicts of interest to declare.

Notes and references

1 (*a*) H. S. Rzepa, *Chem. Rev.*, 2005, **105**, 3697–3715; (*b*) R. Herges, *Chem. Rev.*, 2006, **106**, 3697–3715.
2 The twist points are induced by T_w 180° rotations (T_w = odd number) that can occur in two directions, corresponding to a (+) or (−)helix. Möbius [± T_w] strips have therefore C_2 symmetry and are chiral.
3 (*a*) J. B. Listing, *Abhandlungen der Mathematischen Classe der Königlichen Gesellschaft der Wissenschaften zu Göttingen*, 1861, **10**, 97–182; (*b*) A. F. Möbius, *Berichte über die Verhandlungen der Königlich Sächsischen Gesellschaft der Wissenschaften zu Leipzig*, 1865, **17**, 31–68.
4 S. Tanda, T. Tsuneta, Y. Okajima, K. Inagaki, K. Yamaya and N. Hatakenaka, *Nature*, 2002, **417**, 397–398.
5 O. Cador, D. Gatteschi, R. Sessoli, F. K. Larsen, J. Overgaard, A.-L. Barra, S. J. Teat, G. A. Timco and R. E. P. Winpenny, *Angew. Chem., Int. Ed.*, 2004, **43**, 5196–5200.
6 Z. Geng, B. Xiong, L. Wang, K. Wang, M. Ren, L. Zhang, J. Zhu and Z. Yang, *Nat. Commun.*, 2019, **10**, 4090.
7 Z.-Z. Nie, B. Zuo, M. Wang, S. Huang, X.-M. Chen, Z.-Y. Liu and H. Yang, *Nat. Commun.*, 2021, **12**, 2334.
8 (*a*) M. Stollenz, J. E. Raymond, L. M. Pérez, J. Wiederkehr and N. Bhuvanesh, *Chem. – Eur. J.*, 2016, **22**, 2396–2405; (*b*) J. Arras, A. Calderón-Díaz, S. Lebedkin, S. Gozem, C. D. McMillen, N. Bhuvanesh and M. Stollenz, *Inorg. Chem.*, 2024, **63**, 12943–12957.
9 M. Stollenz, *Chem. – Eur. J.*, 2019, **25**, 4274–4298.
10 The only other example of a triangular mesitylcopper cluster with a single CuMes unit and distances < 2.8 Å between all three metal centers was reported in A. L. Johnson, A. M. Willcocks and S. P. Richards, *Inorg. Chem.*, 2009, **48**, 8613–8622.
11 C. O'Dea, O. Ugarte Trejo, J. Arras, A. Ehnbom, N. Bhuvanesh and M. Stollenz, *J. Org. Chem.*, 2019, **84**, 14217–14226.
12 (*a*) J. Arras, O. Ugarte Trejo, N. Bhuvanesh and M. Stollenz, *Chem. Commun.*, 2022, **58**, 1418–1421; (*b*) J. Arras, O. Ugarte Trejo, N. Bhuvanesh, C. D. McMillen and M. Stollenz, *Inorg. Chem. Front.*, 2022, **9**, 3267–3281.
13 A. Calderón-Díaz, J. Arras, E. T. Miller, N. Bhuvanesh, C. D. McMillen and M. Stollenz, *Eur. J. Org. Chem.*, 2020, 3243–3250.
14 (*a*) S. Gambarotta, C. Floriani, A. Chiesi-Villa and C. Guastini, *J. Chem. Soc., Chem. Commun.*, 1983, 1156–1158; (*b*) E. M. Meyer, S. Gambarotta, C. Floriani, A. Chiesi-Villa and C. Guastini, *Organometallics*, 1989, **8**, 1067–1079; (*c*) Håkansson *et al*. found that $[Cu_4Mes_4]$ (major species), originally believed to be $[Cu_2Mes_2]$ (Ref. 14*b*), and $[Cu_5Mes_5]$ (minor species) coexist in an equilibrium in solution: H. Eriksson and M. Håkansson, *Organometallics*, 1997, **16**, 4243–4244.
15 M. Stollenz and F. Meyer, *Organometallics*, 2012, **31**, 7708–7727.
16 The reaction of $\mathbf{L}^{1}H_2$ and CuMes results in the formation of a greenish tan, weekly orange emitting solid that shows moderate solubility in pyridine. The ^{1}H NMR spectrum in C_5D_5N indicates the presence of multiple species in solution: O. Ugarte-Trejo and M. Stollenz, *unpublished results*.
17 A. Bondi, *J. Phys. Chem.*, 1964, **68**, 441–451.
18 (*a*) H. L. Aalten, G. van Koten, K. Goubitz and C. H. Stam, *J. Chem. Soc., Chem. Commun.*, 1985, 1252–1253; (*b*) H. L. Aalten, G. van Koten, K. Goubitz and C. H. Stam, *Organometallics*, 1989, **8**, 2293–2299.
19 D. M. Knotter, D. M. Grove, W. J. J. Smeets, A. L. Spek and G. van Koten, *J. Am. Chem. Soc.*, 1992, **114**, 3400–3410.
20 M. Niemeyer, *Acta Crystallogr., Sect. E: Struct. Rep. Online*, 2001, **57**, m491–m493.
21 A. L. Keen, M. Doster, H. Hana and S. A. Johnson, *Chem. Commun.*, 2006, 1221–1223.
22 R. A. D. Soriaga, S. Javed and D. M. Hoffman, *J. Cluster Sci.*, 2010, **21**, 567–575.
23 E. Kounalis, M. Lutz and D. L. J. Broere, *Organometallics*, 2020, **39**, 585–592.
24 The original *EE* (*syn*, *syn*) configuration of these bis(amidine) ligands, as found for the majority of their XRD molecular structures (see also Ref. 13), is converted into *EE* (*anti*, *anti*) in the corresponding Cu_4^{I} chain clusters. Since deprotonation to anionic bis(amidinates) results in delocalization of its π electrons and reduced double bond character, the *E*/*Z* and *syn*/*anti* classification refers to CN bonds with a bond order of 1.5 in this case.